

Mottness and magnetism of fermions in a double-well optical lattice

Xin Wang,¹ Qi Zhou,^{1,2} and S. Das Sarma^{1,2}

¹*Condensed Matter Theory Center, Department of Physics,
University of Maryland, College Park, Maryland 20742, USA*

²*Joint Quantum Institute, University of Maryland, College Park, Maryland 20742, USA*

(Dated: October 2, 2022)

We theoretically investigate, using nonperturbative strong correlation techniques, Mott insulating phases and magnetic ordering of two-component fermions in a two-dimensional double-well optical lattice. At filling of two fermions per site, there are two types of Mott insulators, one of which is characterized by spin-1 antiferromagnetism below the Neel temperature. The super-exchange interaction in this system is induced by the interplay between the inter-band interaction and the spin degree of freedom. A great advantage of the double-well optical lattice is that the magnetic quantum phase diagram and the Neel temperature can be easily controlled by tuning the orbital energy splitting of the two-level system. Particularly, the Neel temperature can be one order of magnitude larger than that in standard optical lattices, facilitating the experimental search for magnetic ordering in optical lattice systems.

PACS numbers: 05.30.Fk, 67.85.-d, 71.27.+a, 03.75.-b

There are currently worldwide efforts in studying collective properties of cold atoms either in a single trap or in an optical lattice[1]. A central goal of these studies is to explore novel many-body quantum phases in both bosonic and fermionic systems. While both bosonic and fermionic Mott insulators have been realized in laboratories[2–5], the experimental search for magnetism in optical lattices is currently on-going in many laboratories. Most of these studies have been focusing on the single-band physics so far. For example, it is known that two-component fermions in the lowest band can be used to study spin-1/2 antiferromagnetism[6].

A question then naturally arises: Is it possible to realize more exotic multi-band magnetic systems using cold atoms in optical lattices? Theoretical studies suggest, for example, to explore excited bands in optical lattices for searching novel magnetism[7, 8]. While there are currently experimental efforts along this direction to populate atoms in the excited bands[9, 10], whether one can overcome the finite-life time problem of atoms in excited bands still remains to be seen.

On the other hand, there is a crucial practical issue on the energy and time scale of atoms in optical lattices. Ordinary optical lattices are characterized by extremely small energy scales, which also lead to slow relaxation of lattice systems to equilibrium. For example, the tunneling of the lowest band is about a few nano-Kelvin which corresponds to a time scale of a few tens of milliseconds. The energy scale associated with the super-exchange interaction t^2/U is even smaller since $U > t$ typically. As a result, the Neel temperature of antiferromagnetism in ordinary optical lattices is far too low for experimental observation. Meanwhile, it is also challenging for the system to reach equilibrium because of the long relaxation time. A scheme to enhance the relevant energy scales is therefore very desirable, particularly in the context of the experimental study of many-body magnetism in optical

lattice systems.

In this Letter, we theoretically study quantum magnetism of fermions in a double-well optical lattice. Instead of the usual spin-1/2 magnetic ordering in an ordinary optical lattice, the double-well effectively produces a spin-1 system. The associated magnetism is induced by the inter-band interaction between the lowest two bands, and is a ground state property. Moreover, the characteristic energy scale for observing magnetism can be enhanced by one order of magnitude compared with the spin-1/2 magnetism in ordinary optical lattices. As a result, the magnetism may be much easier to achieve and observe experimentally in the double-well optical lattice.

A double-well optical lattice contains two potential wells, which are separated by a barrier, on each lattice site. A unique advantage is that the band gap between the lowest two bands is tunable[11, 12]. When these two bands are very close to each other, interesting quantum many-body phenomena, which are completely absent in ordinary optical lattices, emerge[12, 13]. We will see that the interplay between the orbital degree of freedom and the fermionic spin lies at the heart of the new physics reported in this Letter. Theoretically it is however challenging to study fermions with spin degrees of freedom in the presence of multiple bands. We employ the dynamical mean-field theory (DMFT) method, and study both the Mott insulating phases and magnetic properties of fermions in a double-well lattice. We show that at filling of two fermions per site, the Mott insulator developed in the system can be either the triplet $(n_s, n_p) = (1, 1)$ states or the admixture $u(2, 0) - v(0, 2)$. For the former case, antiferromagnetic order emerges in the spin-1 channel below the Neel temperature, which should be observable experimentally.

Model. We consider the Hamiltonian containing a tight-binding-band part and an on-site interaction part, characterizing the two lowest bands (labeled by s and

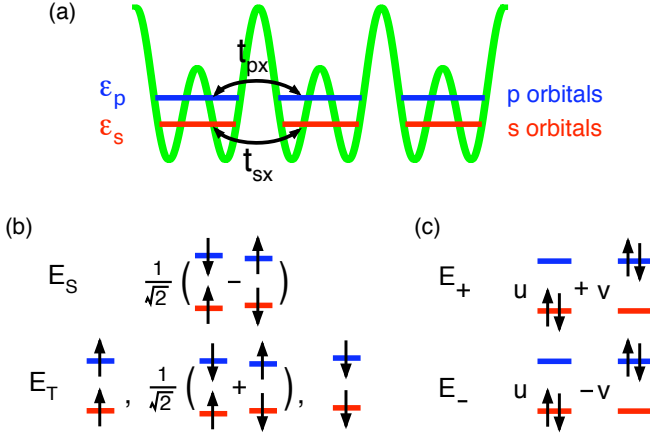


FIG. 1: (Color online) (a) Profile of the double-well potential (the green line) along the x -direction. The s (red lines) and p (blue lines) orbitals are schematically shown. The hopping integrals and energies for $s(p)$ orbitals, $t_{sx}(t_{px})$ and $\epsilon_s(\epsilon_p)$, are indicated. Note that the potential is not double-welled along the y -direction (not shown), where the hopping integrals are t_{sy} and t_{py} correspondingly. (b) $(n_s, n_p) = (1, 1)$ eigenstates in atomic limit, including triplet states with energy E_T and a singlet state with energy E_S . (c) Linear combinations of $(2, 0)$ and $(0, 2)$ states as eigenstates for the Hamiltonian in atomic limit, whose energies are denoted by E_{\pm} . See the text for details.

p respectively) in a symmetric double-well lattice, $H = H_{\text{band}} + H_{\text{int}}$. In the real space, the band part can be written as

$$H_{\text{band}} = \sum_{\mathbf{r}\sigma} \left[(\epsilon_s - \mu) s_{\sigma,\mathbf{r}}^\dagger s_{\sigma,\mathbf{r}} + (\epsilon_p - \mu) p_{\sigma,\mathbf{r}}^\dagger p_{\sigma,\mathbf{r}} \right] + \sum_{\mathbf{r}\sigma} \left(-t_{sx} s_{\sigma,\mathbf{r}}^\dagger s_{\sigma,\mathbf{r}+\mathbf{x}} - t_{sy} s_{\sigma,\mathbf{r}}^\dagger s_{\sigma,\mathbf{r}+\mathbf{y}} - t_{px} p_{\sigma,\mathbf{r}}^\dagger p_{\sigma,\mathbf{r}+\mathbf{x}} - t_{py} p_{\sigma,\mathbf{r}}^\dagger p_{\sigma,\mathbf{r}+\mathbf{y}} + h.c. \right), \quad (1)$$

where $s_{\sigma,\mathbf{r}}^\dagger (p_{\sigma,\mathbf{r}}^\dagger)$ creates a fermion with spin σ on the $s(p)$ orbital of site \mathbf{r} , ϵ_s and ϵ_p are the energies for s and p orbitals, and μ is the chemical potential. The hopping amplitude for s and p orbitals may differ in x and y directions, thus we label them by t_{sx} , t_{sy} , t_{px} , t_{py} respectively.

The interacting part of the Hamiltonian can be written as

$$H_{\text{int}} = \sum_{\mathbf{r}} \left[U_s n_{s\uparrow,\mathbf{r}} n_{s\downarrow,\mathbf{r}} + U_p n_{p\uparrow,\mathbf{r}} n_{p\downarrow,\mathbf{r}} + U_{sp} (n_{s\uparrow,\mathbf{r}} n_{p\downarrow,\mathbf{r}} + n_{s\downarrow,\mathbf{r}} n_{p\uparrow,\mathbf{r}}) - U_{sp} \left(s_{\downarrow,\mathbf{r}}^\dagger p_{\uparrow,\mathbf{r}}^\dagger p_{\downarrow,\mathbf{r}} s_{\uparrow,\mathbf{r}} + p_{\uparrow,\mathbf{r}}^\dagger p_{\downarrow,\mathbf{r}}^\dagger s_{\uparrow,\mathbf{r}} s_{\downarrow,\mathbf{r}} + h.c. \right) \right], \quad (2)$$

where $n_{\alpha\sigma,\mathbf{r}} = \alpha_{i\sigma,\mathbf{r}}^\dagger \alpha_{i\sigma,\mathbf{r}}$ ($\alpha = s, p$) is the number operator for orbital α at site \mathbf{r} , $U_\alpha = \frac{4\pi\hbar^2 a_s}{M} \int d^3x W_\alpha^4(\mathbf{x})$

denotes the intra-band interaction, while $U_{sp} = \frac{4\pi\hbar^2 a_s}{M} \int d^3x W_s^2(\mathbf{x}) W_p^2(\mathbf{x})$ denotes the inter-band interaction, where a_s is the scattering length, M is the mass of the fermion, and $W_\alpha(\mathbf{x})$ is the Wannier wave function for each band. The inter-orbital terms in Eq.(2) characterized by U_{sp} are referred as density-density, spin-exchange and pair-hopping interaction. This model is essentially the rotationally invariant Slater-Kanamori interaction widely studied in transitional metal oxides [14]. The main difference here is that the spin-exchange and pair-hopping are as strong as the inter-orbital density-density interaction. An important parameter which controls the multi-band physics is the energy level splitting between the two levels, defined as $\Delta \equiv \epsilon_p - \epsilon_s$. When Δ is small, interactions between the two orbitals give rise to interesting phenomena, as we discuss below. When Δ becomes very large the physics reduces to that of the single-band model. The Hamiltonian in Eq. (2) has been previously considered for fermions at resonance in an ordinary optical lattice in one-dimension[15]. In our case, the reduced band gap makes the realization of a two-band system more practical in current experiments. Moreover, higher dimensionality of our system gives distinct physical phenomena not accessible in one dimension.

We start from the atomic limit, where the tunneling terms are absent. We are interested in the states at filling of two fermions per site, the schematics of which are shown in Fig. 1(b) and 1(c). When there is one fermion in each orbital, they form triplets which is denoted as $(n_s, n_p) = (1, 1)$, namely, $p_{\uparrow}^\dagger s_{\uparrow}^\dagger |0\rangle$, $\frac{1}{\sqrt{2}} (p_{\uparrow}^\dagger s_{\downarrow}^\dagger + p_{\downarrow}^\dagger s_{\uparrow}^\dagger) |0\rangle$, and $p_{\downarrow}^\dagger s_{\downarrow}^\dagger |0\rangle$, with degenerate energy $E_T = 2(\epsilon_s - \mu) + \Delta$. The singlet state $\frac{1}{\sqrt{2}} (p_{\uparrow}^\dagger s_{\downarrow}^\dagger - p_{\downarrow}^\dagger s_{\uparrow}^\dagger) |0\rangle$ has a higher energy $E_S = 2(\epsilon_s - \mu) + \Delta + 2U_{sp}$. $E_S > E_T$ simply because two fermions interact with each other by s -wave short-range interaction. In the spirit of the Hubbard model, atoms with different spins repel with each other and atoms with the same spin do not interact. On the other hand, the two fermions can also form admixtures $u(2, 0) \pm v(0, 2)$, as shown in Fig. 1(c), due to the pair-hopping interaction. The eigenenergies are $E_{\pm} = 2(\epsilon_s - \mu) + \Delta + \frac{U_p + U_s}{2} \pm \sqrt{\left(\Delta + \frac{U_p - U_s}{2}\right)^2 + U_{sp}^2}$. By controlling Δ in the double-well lattice, E_- can be made either smaller or larger than E_T . Throughout the paper we fix parameters as $t_{sx} = t_{sy} = t_{py} = t$, $t_{px} = 2t$, $U_s = 12t$, $U_p = 14t$, $U_{sp} = 12t$, and vary Δ and the temperature T . Straightforward algebra reveals that at the critical value $\Delta_c = 4t$, $E_- = E_T$.

When the hopping terms are switched on, we employ the single-site DMFT [16] to solve the strongly-correlated interacting lattice fermion problem. The key of the non-perturbative DMFT approximation is the neglecting of momentum dependence of the self-energy: $\Sigma(\mathbf{k}, \omega) \rightarrow \Sigma(\omega)$, which is then solved iteratively from an auxiliary

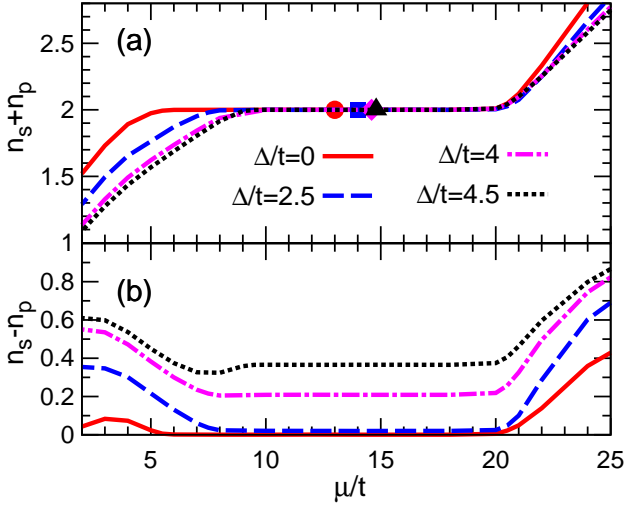


FIG. 2: (Color online) (a) Total occupancy ($n_s + n_p$) versus chemical potential μ , calculated for three different values of Δ . The calculation is done without magnetic order at temperature $T = 0.2t$. $\varepsilon_s = 0$ in this plot. The points (the circle, the square, the diamond and the triangle) indicate the location at approximately the center of the gap for the line with corresponding color, where we study magnetic ordering. (b) The difference in occupancy $n_s - n_p$ plotted at the same μ scale.

quantum impurity problem plus a self-consistency condition. We use the matrix representation of the continuous-time hybridization-expansion quantum Monte Carlo impurity solver [17] prescribed specifically for multi-band interactions. This is a state of the arts highly demanding numerical solution of the strongly interacting multi-band lattice Hubbard model in the context of our double-well optical lattice system.

Mott physics.— There are multiple choices to fill a single lattice site with two fermions, forming different types of Mott insulator. To distinguish them, we have calculated both $n_s + n_p$ and $n_s - n_p$ as functions of μ for different values of Δ , as shown in Fig. 2(a). A Mott insulating gap at filling two is evident for all cases, and there is no qualitative difference in the value of $n_s + n_p$ between different cases. However, the difference in occupancy for the two orbitals ($n_s - n_p$) shows distinct behaviors. For a very large level splitting $\Delta = 4.5t$, $n_s \gg n_p$. This is consistent with the analysis in the previous section for the atomic limit, where each lattice site is filled by the state $u(2,0) - v(0,2)$ and $u \gg v$. In contrast, at small Δ , e.g. as seen in Fig. 2(b) for $\Delta = 2.5t$ and $\Delta = 0$, $n_s \approx n_p$ in the Mott insulating regime. This indicates that on each site the triplet states dominate the ground state. This is also consistent with the atomic limit where the energy of (1,1) states E_T continuously decreases and eventually the (1,1) triplet becomes the ground state with decreasing Δ , as discussed in the previous section.

For the large Δ case, the magnetism is manifestly absent and the ground state continuously connects to the trivial band insulator in the lowest band of an ordinary optical lattice, when the energy splitting Δ increases toward infinity. For small Δ , however, a magnetization of spin-1 may arise from the triplet states on a single lattice site. As a result, the physics of magnetic ordering in double-well lattices at filling two is far richer than that in standard optical lattices.

Magnetic order.— When the (1,1) states dominate the on-site Fock states for small Δ , the interacting Hamiltonian can be mapped to a spin-1 Heisenberg model, which can be written as

$$H_{\text{eff}} = \sum_{\mathbf{r}} (J_x \mathbf{S}_{\mathbf{r}} \cdot \mathbf{S}_{\mathbf{r}+\mathbf{x}} + J_y \mathbf{S}_{\mathbf{r}} \cdot \mathbf{S}_{\mathbf{r}+\mathbf{y}}), \quad (3)$$

where

$$J_x = \frac{2t_{sx}^2}{U_s + U_{sp}} + \frac{2t_{px}^2}{U_p + U_{sp}}, \quad J_y = \frac{2t_{sy}^2}{U_s + U_{sp}} + \frac{2t_{py}^2}{U_p + U_{sp}}, \quad (4)$$

$\mathbf{S}_{\mathbf{r}} = A^\dagger \boldsymbol{\Sigma} A$ is a spin-1 operator, $\boldsymbol{\Sigma}$ is the spin-1 Pauli matrices, and $A = (\Psi_1^\dagger, \Psi_0^\dagger, \Psi_{-1}^\dagger)^T$ are creation operators for the triplet states $p_\uparrow^\dagger s_\uparrow^\dagger |0\rangle$, $\frac{1}{\sqrt{2}} (p_\uparrow^\dagger s_\downarrow^\dagger + p_\downarrow^\dagger s_\uparrow^\dagger) |0\rangle$, and $p_\downarrow^\dagger s_\downarrow^\dagger |0\rangle$. Physically, the spin-exchange terms in Eq. (3) come from the exchange of fermions with different spins between the nearest neighbor sites in either of the two orbitals. Both orbitals contribute to the spin-exchange terms in the effective Hamiltonian.

In the one-dimensional case, Eq. (3) has previously been derived in Ref. [15]. For that case, it has been known that the one-dimensional spin-1 chain does not have any magnetic order, but rather the Haldane phase. Nevertheless, a two-dimensional spin-1 system can develop antiferromagnetic ground states [18–20]. Therefore, one expects to see antiferromagnetic spin ordering in a double-well optical lattice when the gap Δ is small and the temperature is low.

To characterize the magnetization, we define $m = |n_{s\uparrow} - n_{s\downarrow} + n_{p\uparrow} - n_{p\downarrow}|$ and solve the full Hamiltonian $H = H_{\text{band}} + H_{\text{int}}$. The results for m as a function of the temperature for different Δ are shown in Fig. 3(a). Clearly, the magnetization arises below the Neel temperature (denoted by T^{Neel}) and saturates to its maximum value as the temperature approaches zero. For $\Delta = 0$, the antiferromagnetic ordering is most pronounced: it has the highest Neel temperature $T^{\text{Neel}} \simeq 0.37t$. As Δ is increased, the magnetization drops faster as T increases, and the Neel temperature decreases. For a relatively large $\Delta = 4.5t$, $T^{\text{Neel}} \simeq 0.21t$. Note that this value of Δ is already above the critical value $\Delta_c = 4t$ in the atomic limit where $u(2,0) - v(0,2)$ is the ground state. This indicates that the correlation between nearest neighbor sites enhances the threshold of Δ_c for a finite m to emerge.

To give a broader picture, we show in Fig. 3(b) a color plot of the magnetization on a plane, of which the axes

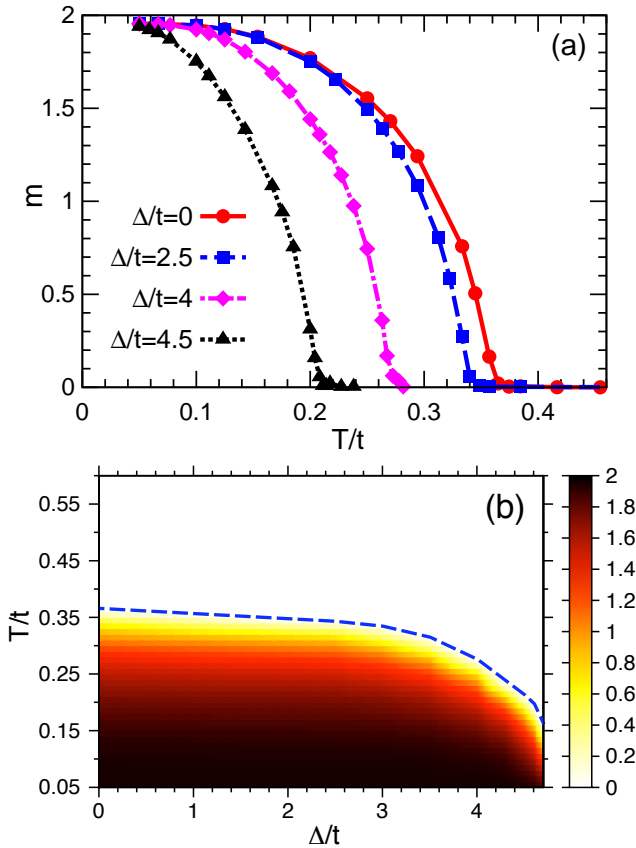


FIG. 3: (Color online) (a) Total magnetization $m = |n_{s\uparrow} - n_{s\downarrow} + n_{p\uparrow} - n_{p\downarrow}|$ versus temperature, for four selective values of Δ . The chemical potential is selected at approximate center of the gap (see Fig. 2). (b) Color plot of the magnetization on the Δ - T plane. In the white regime there is no magnetic order, while for low T the magnetization reaches the maximum value, indicated as dark colors. The Neel temperature is shown as blue dashed lines separating colored and white regimes. Note that the y -axis does not start from zero: it starts from the lowest temperature $T = 0.05t$ reached in the DMFT calculation.

are the energy level splitting Δ and the temperature T . The blue dashed line, separating colored and white regimes, indicates the Neel temperature, above which no magnetic order is present. The dark color shown near the lowest accessible temperature $T = 0.05t$ in our simulations characterizes the saturation of the magnetization to its maximum value. As the temperature is increased to intermediate values, the color turns to red, indicating a moderate drop of the magnetization. When the temperature is close to the Neel temperature, the magnetization drops rapidly, as can be seen from the narrow yellow edge. A close examination of the Neel temperature reveals that it drops relatively slowly for $\Delta < \Delta_c$, but very rapidly for $\Delta > \Delta_c$. This is consistent with the qualitative atomic picture. For $\Delta \rightarrow \infty$, the magnetic

ordering and the corresponding Neel temperature would eventually vanish. But the remarkable thing we have shown is that they would survive at least for Δ immediately larger than Δ_c , which would relieve the restriction posed on experiments in order to achieve the magnetic ordering. An alternative way to appreciate these results is that both m and T^{Neel} are tunable by controlling Δ , which has obvious important experimental implications.

Enhancement of super-exchange interaction.- The increase of J [cf. Eqs. (3) and (4)] in a double-well lattice comes from two sources. First, as seen from Eq. (4), in addition to t_s , t_{px} and t_{py} also enter the expression for the super-exchange interaction J . Second, t_{sx} itself is significantly enhanced in a double-well optical lattice. It has been shown that t_{sx} can be increased by one order of magnitude at a given lattice depth for some realistic experimental parameters, while t_{px} remains more or less the same[12]. Thanks to the potential barrier in the center of each lattice site of a double-well lattice, the Wannier wave function of the lowest band spreads its weight toward the edge of the corresponding unit cell. Consequently, though the onsite interaction strength changes only slightly, the overlap of the Wannier wave functions between adjacent sites is greatly enhanced compared to that in ordinary optical lattices, thus greatly enhancing the tunneling strength. As a result, the Neel temperature can be strongly enhanced, easily by one order of magnitude. The larger energy scale associated with the tunneling and super-exchange interaction will also help to reach equilibrium faster in the strongly interacting region.

Conclusion.- Using non-perturbative ‘DMFT with continuous-time quantum impurity solver’ direct numerical techniques, we study two-component fermions in a two-dimensional double-well square optical lattice, with two interacting orbitals on each site. The Mott insulator at filling two is constituted either by triplet $(n_s, n_p) = (1, 1)$ or an admixture $u(2, 0) - v(0, 2)$. For the one associated with the triplets, antiferromagnetic order emerges in the spin-1 channel below the Neel temperature, which is determined by the energy splitting between the two orbitals and the tunneling amplitude. We establish that, as t_p contributes to J and t_{sx} is significantly enlarged in double-well lattices, the Neel temperature can be one order of magnitude larger than that of the one-band system in ordinary optical lattices, thus perhaps enabling the direct experimental observation of the elusive Neel antiferromagnetism in cold atomic systems. Our work, utilizing the state of the arts numerical strong correlation quantum techniques, should facilitate the search of magnetic order in optical lattice systems.

Acknowledgements: We thank M. Cheng and A. J. Millis for discussions. This work is supported by JQI-NSF-PFC, ARO-DARPA-OLE, JQI-ARO-MURI, and JQI-AFOSR-MURI. The impurity solver in the DMFT procedure is based on a code primarily developed by P. Werner,

and uses the ALPS library[21].

-
- [1] I. Bloch, Nature Phys. **1**, 23 (2005).
 - [2] M. Greiner, O. Mandel, T. Esslinger, T.W. Hänsch, and I. Bloch, Nature **415**, 39 (2002).
 - [3] N. Gemelke, X. Zhang, C.-L. Hung, and C. Chin, Nature **460**, 995 (2009).
 - [4] R. Jördens, N. Strohmaier, K. Günter, H. Moritz, and T. Esslinger, Nature **455**, 204 (2008).
 - [5] U. Schneider, L. Hackermüller, S. Will, T. Best, I. Bloch, T. A. Costi, R. W. Helmes, D. Rasch, and A. Rosch, Science **322**, 1520 (2008).
 - [6] W. Hofstetter, J. I. Cirac, P. Zoller, E. Demler, and M. D. Lukin, Phys. Rev. Lett. **89**, 220407 (2002).
 - [7] C. Wu, Phys. Rev. Lett. **100**, 200406 (2008).
 - [8] S. Zhang, H.-h. Hung, and C. Wu, Phys. Rev. A **82**, 053618 (2010).
 - [9] T. Müller, S. Fölling, A. Widera, and I. Bloch, Phys. Rev. Lett. **99**, 200405 (2007).
 - [10] G. Wirth, M. Ölschläger, and A. Hemmerich, Nature Phys. **7**, 147 (2011).
 - [11] J. Larson, A. Collin, and J.-P. Martikainen, Phys. Rev. A **79**, 033603 (2009).
 - [12] Q. Zhou, J. V. Porto, and S. Das Sarma, Phys. Rev. B **83**, 195106 (2011).
 - [13] Q. Zhou, J. V. Porto, and S. Das Sarma, arXiv:1105.0012 (2011).
 - [14] X. Wang, H. T. Dang, and A. J. Millis, Phys. Rev. B **84**, 014530 (2011); **84**, 073104 (2011); M. J. Han, X. Wang, C. A. Marianetti, and A. J. Millis, arXiv:1105.0016.
 - [15] A. F. Ho, Phys. Rev. A **73**, 061601 (R) (2006).
 - [16] A. Georges, G. Kotliar, W. Krauth, and M. J. Rozenberg, Rev. Mod. Phys. **68**, 13 (1996); G. Kotliar, S. Y. Savrasov, K. Haule, V. S. Oudovenko, O. Parcollet, and C. A. Marianetti, *ibid.* **78**, 865 (2006).
 - [17] P. Werner and A. J. Millis, Phys. Rev. B **74**, 155107 (2006); E. Gull, A. J. Millis, A. I. Lichtenstein, A. N. Rubtsov, M. Troyer, and P. Werner, Rev. Mod. Phys. **83**, 349 (2011).
 - [18] Y. J. Kim and R. J. Birgeneau, Phys. Rev. B **62**, 6378 (2000).
 - [19] T. Sakai and M. Takahashi, J. Phys. Soc. Jpn. **58**, 3131 (1989).
 - [20] Y. Q. Wang, G. S. Tian, and H. Q. Lin, Phys. Rev. B **67**, 064408 (2003).
 - [21] A.F. Albuquerque *et al.*, J. Magn. Magn. Mater. **310**, 1187 (2007); <http://alps.comp-phys.org/>.